

Supplementary material

Vortex Flow of Downwind Sails

A . Experimental setup images

A set of images of the experimental setup is presented in Figure 1.

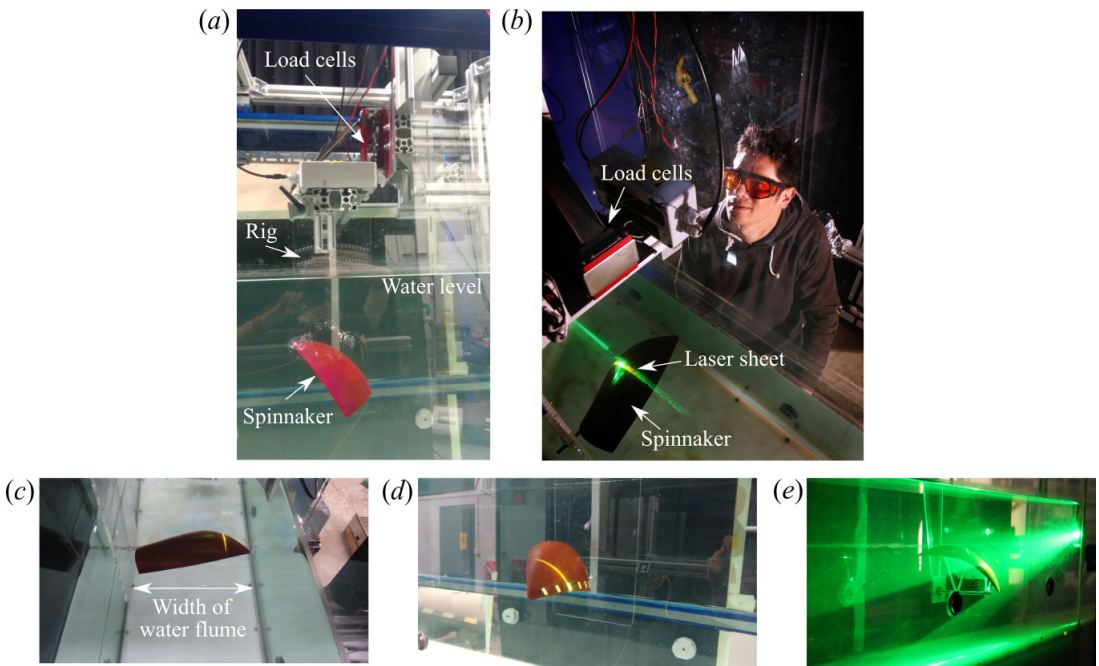


Figure 1. Images of the experimental setup showing (a) a side view with the spinnaker and the key components of the rig highlighted, (b) a bird's eye view with the laser sheet illuminating plane C of the spinnaker, (c) the spinnaker model spanning the width of the water flume, (d) the spinnaker model during the alignment of the laser sheet, when markers are placed at the leech (trailing-edge) to indicate the test planes, and (e) a wide-shot of the spinnaker illuminated by the laser sheet.

B . PIV uncertainty

The interval between time frames was set to ensure that the in-plane motion was limited to one quarter of the linear dimension of the interrogation window, as recommended by Adrian (1997). Correlation peaks values were identified in the range of 0.4-0.8. A decreasing adaptive correlation window (described in §2.6 of the main manuscript) was used to reduce PIV uncertainty (Baum et al., 2014). The PIV error

01
02
03
04
05
06
07
08
09
10
11
12
13
14
15
16
17
18
19
20
21
22
23
24
25
26
27
28
29
30
31
32
33
34
35
36
37
38
39
40
41
42
43
44
45
46
47
48
49
50
51
52

was quantified as follows. The total PIV error can be defined as $\epsilon_{PIV} = \epsilon_{rms} + \epsilon_{bias}$, where ϵ_{rms} is the random error and ϵ_{bias} is the bias error. Following one of the methods presented in Raffel et al. (2018), the random error was estimated by taking a velocity measurement of the stationary fluid, where the water tunnel was left quiescent for sufficient time to ensure that any turbulent motion was dissipated. Figure 2 shows the probability density function of the estimated streamwise and normal flow velocities (u and v , respectively) computed with 250 images, each with 25,000 velocity vectors. Both distributions are normal and the 95% confidence interval is used as estimate of the random error, which is $\epsilon_{rms} = 0.01U_\infty$ for both u and v . The bias error (ϵ_{bias}) could not be quantified. However, Wieneke (2015) found that it is usually smaller than the random error even for strong peak locking. Because our correlation peaks did not indicated peak locking and because of the post-processing techniques mentioned above, we conservatively consider the bias error equal to the random error. Hence the PIV total error is estimated to be lower than $0.02U_\infty$ for both u and v .

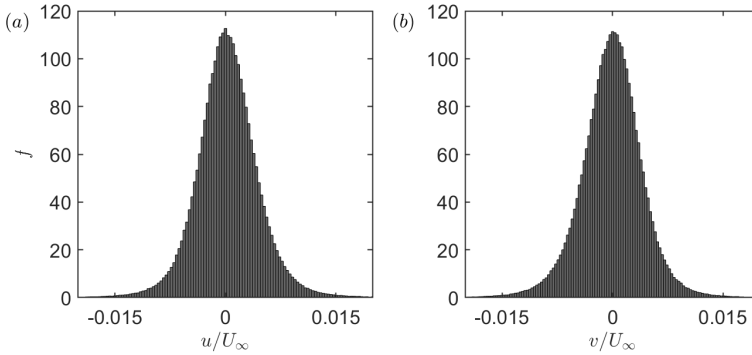


Figure 2. Probability density distribution (f) of the measured u and v velocity components of a stationary flow field (i.e. the actual velocity is zero). These measured velocities are representatives of the random PIV error and thus the velocities are nondimensionalised by the mean velocity U_∞ at which the sail models were tested.

C . Vorticity uncertainty

The out-of-plane vorticity component is given by

$$\omega_z = \frac{\partial v}{\partial x} - \frac{\partial u}{\partial y}. \quad (1)$$

With a central difference scheme, vorticity can be approximated as

$$\omega_z = \frac{1}{2d} [v(x+d, y) - v(x-d, y) - u(x, y+d) + u(x, y-d)], \quad (2)$$

where d is the distance between uniformly distributed grid points. By propagation of uncertainties (Taylor, 1997), if various quantities x, \dots, w are measured with small uncertainties $\delta x, \dots, \delta w$ and the measured values are used to calculate some quantity q as a sum or subtraction, then the uncertainties in x, \dots, w cause an uncertainty in q as follows:

$$\delta q = \sqrt{\left(\frac{\partial q}{\partial x}\right)^2 (\delta x)^2 + \dots + \left(\frac{\partial q}{\partial w}\right)^2 (\delta w)^2}. \quad (3)$$

Hence, the vorticity uncertainty is given by

$$\delta\omega_z^2 = 2 \left(\frac{1}{2d} \right)^2 [\delta u^2 + \delta v^2]. \quad (4)$$

The vorticity uncertainty can be reduced by using every second grid point for the finite difference approximation (Sciaccitano and Wieneke, 2016), such that

$$\omega_z = \frac{1}{4d} [v(x+2d, y) - v(x-2d, y) - u(x, y+2d) + u(x, y-2d)], \quad (5)$$

and the vorticity uncertainty is

$$\delta\omega_z^2 = 2 \left(\frac{1}{4d} \right)^2 [\delta u^2 + \delta v^2]. \quad (6)$$

From the estimate of the PIV error discussed in Section B, the velocity uncertainties are $|\delta u| = |\delta v| \leq 0.02U_\infty$. We used two different spatial resolutions: for the smaller field of view (e.g. used in §3.2), $d = 0.013c$ and thus the uncertainty of the vorticity is $\delta\omega_z \leq 1U_\infty/c$, whilst for the wider field of view used (e.g. used in §3.4), $d = 0.004c$ and the uncertainty of the vorticity is $\delta\omega_z \leq 3U_\infty/c$. We note that the finer resolution used in §3.4 is sufficient to perform the vorticity flux analysis of §3.5.

D . Force uncertainty

The uncertainties in the lift and drag coefficients, δC_L and δC_D , were determined through a susceptibility analysis. We illustrate the uncertainty methodology with C_L , where the measurement uncertainty is given by

$$\delta C_L = \sqrt{\left[\frac{\partial C_L}{\partial A} \delta A \right]^2 + \left[\frac{\partial C_L}{\partial L} \delta L \right]^2 + \left[\frac{\partial C_L}{\partial \rho} \delta \rho \right]^2 + \left[\frac{\partial C_L}{\partial U} \delta U \right]^2}, \quad (7)$$

where δA , δL , $\delta \rho$ and δU are changes in A , L , ρ and U , respectively. We recall that A is the area of the sail, L is the lift force, ρ is the fluid density and U is the freestream velocity. To compute δC_D , C_L and L are replaced by C_D and D in equation 7 of the supplementary material document.

In our experiment $\delta A = 0 \text{ m}^2$, since the area of the sail remained constant. Subsequently, δL and δD were obtained by repeating the force calibration of the rig and the sails three times. The calibration consisted in obtaining voltage versus force plots by applying known weights to the load cells in the corresponding direction of L and D . The calibration was repeated three times because the repeatability of the measurement was tested with the three different twisted sails. This yielded $\delta L = 0.04 \text{ N}$ and $\delta D = 0.003 \text{ N}$. Further details of the calibration can be accessed in Arredondo-Galeana (2019). Density uncertainty $\delta \rho$ was determined by measuring the temperature of the water inside the flume, at one hour intervals. The maximum change of temperature measured was $\Delta T = 0.5^\circ \text{ C}$, which accounted for a change of $\delta \rho \leq 0.002 \text{ kg/m}^3$. Lastly, $\delta U \leq 0.001 \text{ m/s}$, which was measured by comparing one hour interval measurements of free stream velocity 1 m upstream of the sail.

Considering that at $\eta = 0^\circ$, $C_L = 1.3$ and $C_D = 0.5$ for sail S_1 , our analysis yields uncertainties of 5% for C_L and 1% for C_D . Applying error propagation rules (Taylor, 1997) at the same η , we obtain uncertainties of 10% for the driving force coefficient C_{DF} , 6% for the side force coefficient C_{SF} , 3% for lift to drag ratio C_L/C_D and 4% for C_L^2 . Error bars are added to the measurements of sail S_1 in figure 4 of the main manuscript.